

# Decoding of Gold-Coded Space-Frequency Block Codes: QRM-MLD vs. Sphere Decoding

Bijan ROHANI<sup>†</sup> and Kambiz HOMAYOUNFAR<sup>‡</sup>

Phybit Inc.

<sup>†</sup> 120 Lower Delta Road  
Cendex Centre #10-10, SINGAPORE

<sup>‡</sup> Higashi Gotanda AM Building  
2-3-3 Higashi Gotanda, Shinagawa  
Tokyo 141-0022 JAPAN

E-mail: {bijan, kambiz}@phybit.com

**Abstract** The Golden Code (GC) is a “perfect code” for the 2×2 MIMO configuration. It has already been adopted for WiMAX in the form of a Space-Frequency Block Code. The challenge with perfect codes in general and GC is in particular is the decoder. The most popular decoder for perfect codes is the Sphere Decoder (SD). But SD can become very complex as the modulation constellation and the MIMO size increase. In this paper we demonstrate how the GC can be decoded by QRM-MLD, hence paving the way for adoption of perfect codes in LTE and advanced LTE without major modifications to the transmitter and receiver.

**Key words** Golden code, Perfect code, Sphere Decoder, QRM-MLD, LTE

## 1. Introduction

Multiple-Input Multiple-Output (MIMO) antenna systems have been long used for improving the reliability of radio links by providing some spatial diversity between the transmitting and receiving antennas in the presence of Rayleigh fading. In recent years, however, we have witnessed another facet of MIMO systems, i.e., spatial multiplexing, gain popular attention. We briefly describe these features of MIMO systems with reference to a 2×2 MIMO system.

A 2×2 MIMO arrangement has been depicted in Figure 1. Here, the channel impulse responses between each transmit antenna  $j$  and the receive antenna  $i$  has been shown as  $\mathbf{h}_{ij}$ ;  $i, j = 1, 2$ , where  $\mathbf{h}_{ij}$  are modeled as complex-valued i.i.d. Gaussian random variables<sup>1</sup>.

If the MIMO arrangement of Figure 1 is used for spatial diversity, both Tx antennas transmit the same information. In this case, the MIMO channel provides 4 independent

radio paths between the Tx and the Rx. As such, probability of outage because of all 4 radio paths falling in a deep fade simultaneously is greatly reduced. In general, in a high signal-to noise ratio (SNR) regime,  $P_e \propto SNR^{-d}$  where  $P_e$  is the probability bit error and  $d$  is the diversity gain of the multi antenna system. In the case of Figure 1, with a maximum diversity gain  $d = 4$ , the outage probability is expected to drop off with a slope 4-times

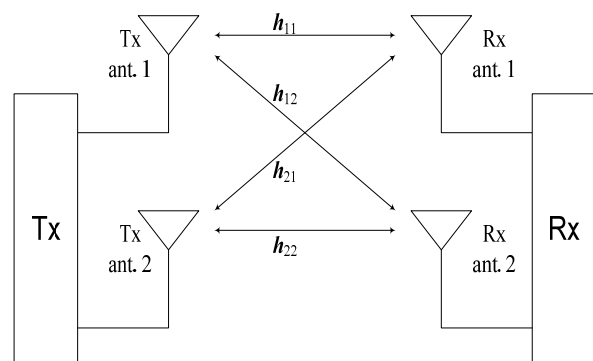


Figure 1 The block diagram of a 2×2 MIMO arrangement.

<sup>1</sup> This is assuming sufficient separation among antennas for each Tx-Rx radio link to be considered independent of others.

steeper than in the case of a Single-Input Single-Output (SISO) system with  $d = 1$ . In general, it has been shown that the diversity gain of a  $n_T \times n_R$  MIMO system is  $d = n_T n_R$ .

Alternatively, the MIMO system in Figure 1 can be configured to deliver more capacity through spatial multiplexing i.e. sending independent streams of data from each Tx antenna. In this case, the transmitted signals from the two Tx antennas interfere with each other at the receiving side. Provided the interference from the other antenna can be estimated accurately enough, the two transmitted data streams can be detected by applying the maximum-likelihood principle (ML) or its sub-optimal variants at the receiver. The achievable transmission rate  $R$  in bits/s/Hz in a high SNR regime is given by  $R = \log_2 SNR^r$  where  $r$  is the spatial multiplexing gain. For the example shown in Figure 1, the spatial multiplexing gain is  $r = 2$ . In general, it has been shown that a spatial multiplexing gain of  $r = \min(n_T, n_R)$  is achievable for a  $n_T \times n_R$  MIMO system.

Spatial diversity is desirable in low SNR regimes so the outage probability can be improved. But, it is a waste of hardware at high SNR, especially if the extra hardware can be used for increasing throughput by spatial multiplexing. This is what spurred great interest in space-time block codes (STBC). These codes bring together the abilities of MIMO systems to provide spatial diversity and spatial multiplexing in a single scheme. They make it possible to trade off diversity with spatial gain depending on the prevailing channel conditions.

A powerful class of STBC is the Perfect Codes (PC). These achieve the diversity-multiplexing tradeoff. They are the optimal space-time codes for  $n_T = n_R = 2, 3, 4$ , and 6 MIMO systems since they achieve full-rate and full-diversity [1].

Sphere decoders (SD) have been widely used for detecting PCs. Although the SD is a powerful research tool for investigating the performance of perfect codes, it is not an attractive choice for practical applications because of several limitations. For example, the SD does not lend itself to parallel implementation which is a desirable feature for VLSI implementations. Additionally, its computational complexity and decoding latency are not fixed for a given combination of coding and modulation. Further to these, computing soft decision outputs from SD is not straightforward.

In this paper, we investigate decoding of PCs with QRM-MLD MIMO detection scheme. This MIMO detection scheme has already been very well researched and methods for improving its computational efficiency have been investigated.

We describe the Golden Code (GC) which is the perfect code for  $2 \times 2$  MIMO systems in Section 2. Next, we present the simulation model in Section 3, followed by some simulation results in Section 4. We conclude with some remarks in Section 5.

## 2. The Golden Code

The Golden Code is the optimum STBC for  $2 \times 2$  MIMO antenna systems adopted for WiMAX [2] and 802.11n [3]. It can achieve the maximum diversity order of  $d = 4$  as well as being capable of a spatial multiplexing gain of  $r = 2$ . Moreover, the GC permits diversity-multiplexing tradeoff depending on channel conditions. In a high SNR regime, a higher modulation order can be used for improved spectral efficiency at the price of reduced diversity. The opposite is done to improve reliability in low SNRs. The spectral efficiency of the GC for M-QAM is  $R = 2 \log_2 M$  b/s/Hz.

With GC, a codeword  $\mathbf{X}$  is derived from four M-QAM symbols  $\mathbf{s}_i; i = 1, 2, 3, \text{ and } 4$  as follows

$$\mathbf{X} = \frac{1}{\sqrt{5}} \begin{bmatrix} \alpha(\mathbf{s}_1 + \mathbf{s}_2\theta) & \alpha(\mathbf{s}_3 + \mathbf{s}_4\theta) \\ i\bar{\alpha}(\mathbf{s}_3 + \mathbf{s}_4\bar{\theta}) & \bar{\alpha}(\mathbf{s}_1 + \mathbf{s}_2\bar{\theta}) \end{bmatrix} \quad (1)$$

where  $i = \sqrt{-1}$ ,  $\theta = (1 + \sqrt{5})/2$ ,  $\bar{\theta} = (1 - \sqrt{5})/2$ ,  $\alpha = 1 + i - i\theta$ , and  $\bar{\alpha} = 1 + i - i\bar{\theta}$  are the Golden code constants. These determine the degree of correlation between transmitted signals in time and space.

## 3. System Model

A simplified block diagram of our simulation model has been shown in Figure 2. We have chosen an orthogonal frequency division multiplex (OFDM) MIMO system in line with many of the current and future wireless standards such as the WiMAX, 802.11a/e/g/n, and the 3G LTE. In the model shown in Figure 2, the blocks of binary data are first encoded using a standard turbo code. The resulting coded bits are mapped to 16QAM symbols  $\mathbf{s}_i; i = 1, 2, \dots$  before applying the Golden code according to (1). The GC codewords  $\mathbf{X}$  are next split into two parallel

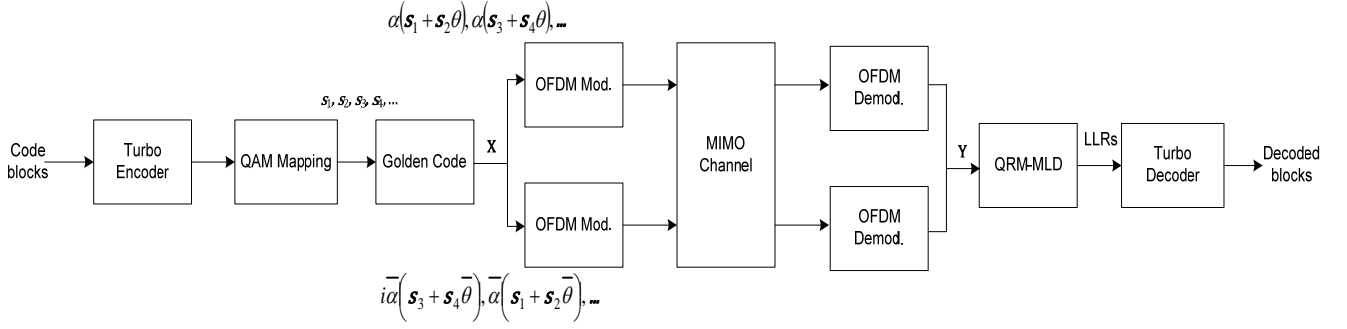


Figure 2 The simplified block diagram of the OFDM-MIMO simulation model.

streams for transmission over the  $2 \times 2$  MIMO channel. However, before transmission, the codewords are modulated by two parallel OFDM modulators. In this case, the successive time slots are mapped to successive OFDM subcarriers. This mapping transforms temporal signal diversity into frequency signal diversity. As such, the STBC is converted to a space-frequency block code (SFBC). Since the subcarrier spacing is chosen to ensure independent Rayleigh fading in adjacent subcarrier, SFBC is effectively equivalent to STBC.

At the receiving side, the signal from the  $2 \times 2$  MIMO channel is first demodulated to give

$$\mathbf{Y} = \mathbf{H}\mathbf{X} + \mathbf{n} \quad (2)$$

Here  $\mathbf{H} = [\mathbf{h}_{ij}]_{2 \times 2}$  is the  $2 \times 2$  MIMO channel with  $\mathbf{h}_{ij} \sim \mathcal{CN}(0,1)$ , and  $\mathbf{n} = [\mathbf{n}_{ij}]_{2 \times 2}$  is the additive white noise with  $\mathbf{n}_{ij} \sim \mathcal{CN}(0, N_o)$  and average power  $N_o$ .

The received signal in (2) can be detected by first vectorizing  $\mathbf{Y}$  as follows,

$$\mathbf{Y}' = \mathbf{H}'\mathbf{R}\mathbf{X}' + \mathbf{n}' \quad (3)$$

where  $\mathbf{X}' = [\mathbf{s}_1 \ \mathbf{s}_2 \ \mathbf{s}_3 \ \mathbf{s}_4]^T$  is the vector of the transmitted symbols, and

$$\mathbf{R} = \begin{bmatrix} \alpha & \alpha\theta & 0 & 0 \\ 0 & 0 & \bar{\alpha} & \bar{\alpha}\bar{\theta} \\ 0 & 0 & \alpha & \alpha\theta \\ \bar{\alpha} & \bar{\alpha}\bar{\theta} & 0 & 0 \end{bmatrix} \quad (4)$$

is the GC encoding matrix. Additionally

$$\mathbf{H}' = \begin{bmatrix} \mathbf{H} & \mathbf{0} \\ \mathbf{0} & \mathbf{H} \end{bmatrix} \quad (5)$$

is the equivalent channel matrix. This is analogous to a

$4 \times 4$  MIMO channel comprising of the  $2 \times 2$  channel  $\mathbf{H}$  and its duplicate. Additionally, the two sets of  $2 \times 2$  channels do not interfere with one another as manifested by the off-diagonal zero matrices.

In our investigation we assumed perfect knowledge of the channel matrix  $\mathbf{H}$ , however, in practice this is estimated with the aid of pilot or reference symbols.

The ML soft detection of (2) is performed by calculating the log-likelihood ratio (LLR) values  $\lambda_{i,k}$  according to

$$\lambda_{i,k} = \min_{\mathbf{X}' \in \mathcal{X}_{i,k}^0} \|\mathbf{Y}' - \mathbf{H}'\mathbf{R}\mathbf{X}'\|^2 - \min_{\mathbf{X}' \in \mathcal{X}_{i,k}^1} \|\mathbf{Y}' - \mathbf{H}'\mathbf{R}\mathbf{X}'\|^2 \quad (6)$$

where  $\|\cdot\|$  denotes the Euclidean distance, and

$$\mathcal{X}_{i,k}^b = \{\mathbf{X}': \ell_k(\mathbf{s}_i) = b\} \quad (7)$$

represents the set of all transmitted uncoded vectors  $\mathbf{X}' = [\mathbf{s}_1 \ \mathbf{s}_2 \ \mathbf{s}_3 \ \mathbf{s}_4]^T$  whose  $k^{\text{th}}$  bit of the  $i^{\text{th}}$  symbol given by  $\ell_k(\mathbf{s}_i)$  is  $b = 0$  or  $1$ .

Equations (3) – (7) can be used as the basis for the detection of the GC by the SD or other ML algorithms and their suboptimum variants. It is easy to see that  $\mathbf{H}'\mathbf{R}$  in (6) is analogous to a  $4 \times 4$  MIMO channel for the transmission of uncoded vector  $\mathbf{X}'$ . As such, a conventional QRM-MLD for a  $4 \times 4$  MIMO detection can be conveniently used for the soft-detection in (6). In the following Section, we investigate decoding the GC by the QRM-MLD. We do not elaborate on the detection algorithm any further and refer the readers to [4].

## 4. Simulation Results

Some of the main simulation parameters of the model of Figure 2 are summarized in Table 1.

We first determined the number of surviving symbol replica candidates (SSRC) for the QRM-MLD to achieve the same performance as the SD assuming hard-decision decoding. For convenience, we increased the number of SSRC in powers of 2 while keeping a uniform number of survivors for stages 2, 3, and 4. The results of the simulations are shown in Figure 3. As can be seen in Figure 3, the QRM-MLD with SSRC of (16, 256, 256, 256) could achieve identical performance as the SD. We used this SSRC for the remaining simulations.

Next we verified the achievable diversity gain as a result of space diversity by comparing the BER performance of the system with and without the Golden code using the QRM-MLD. The results are shown in Figure 4. The slopes of the two BER curves at high SNR give the diversity gain of each scheme. In this case, the scheme with the GC shows a diversity gain  $d$  larger than the scheme without the GC.

Finally, we included turbo channel coding in the simulation. The encoder was a standard rate-1/3 parallel concatenated convolution code with parameters as shown in Table 2. We used a Max-Log-MAP decoder with 8 decoding iterations. The results are shown in Figure 5. As it can be observed from the results, a coding gain in excess of 6 dB was achieved at BER= $10^{-4}$ .

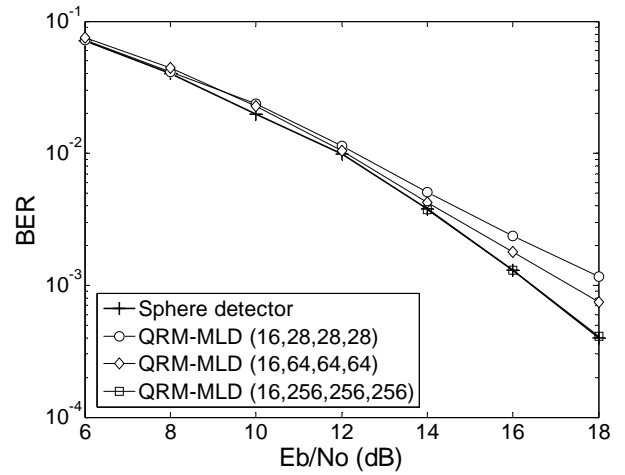


Figure 3 Performance of QRM-MLD for increasing number of SSRC.

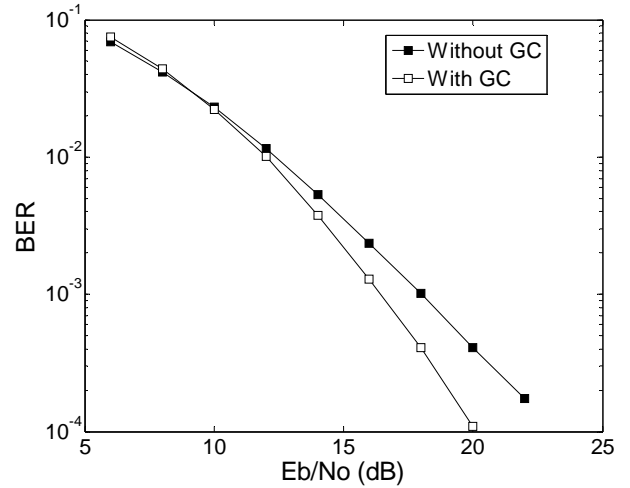


Figure 4 Diversity gain of the scheme with and without GC.

Table 1 Simulation parameters

MIMO antennas	2x2
Symbol modulation	16QAM
OFDM parameters	Number of occupied subcarriers : 601 FFT size: 1024 Number of OFDM symbols per subframe: 6 Subframe duration: 2 ms Sampling interval (Ts): 1/3.84x10 <sup>6</sup> sec.
Channel model	6-path exponentially decaying Rayleigh fading Path gains : [0, -2, -4, -6, -8, -10] dB Path delays : [0, 3, 6, 9, 12, 14] xTs Max. Doppler Frequency : 100Hz
Noise	AWGN
Channel estimates	Perfect
Synchronization	Ideal

Table 2 Turbo encoder parameters

Generator polynomial	$\left[1, \frac{1+D+D^2}{1+D^2+D^3}\right]$
Code rate	1/3
Number of states	8
Turbo code block size	14400 bits

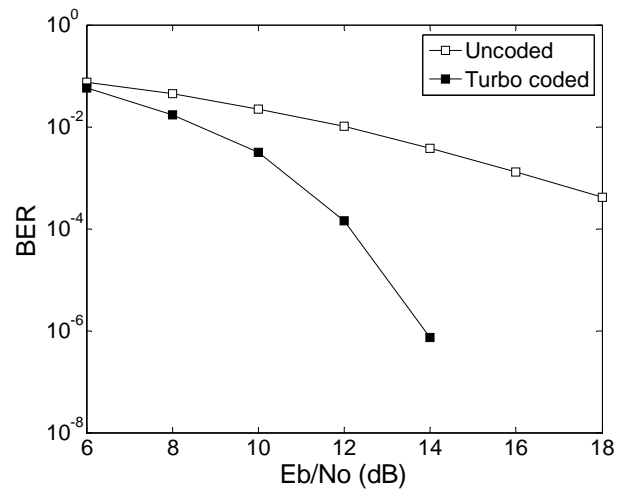


Figure 5 Performance comparison of turbo coded and uncoded schemes with GC.

## 5. Conclusions

Considering that the QRM-MLD is a candidate for MIMO detection for the LTE and advanced LTE, in this paper we have shown the QRM-MLD can be used as an alternative to the sphere decoder for MIMO detection in conjunction with the Golden code STBC. In our study we used the QRM-MLD with SSRC of (16, 256, 256, 256). We recognize that the SSRC can be further refined to achieve the same performance with lower number of survivors by exhaustive simulations. We also recognize that the computational complexity of the QRM-MLD can be significantly reduced by methods such as adaptive selection of surviving symbol replicas, or computationally efficient distance metric. But these were not considered in our preliminary study presented here.

## 5. References

- [1] F. Oggier, G. Rekaya, J. -C. Belfiore, and E. Viterbo, "Perfect Space-Time Block Codes", IEEE Trans. on Info. Theory, Vol. 52, pp. 3885 - 3902 Sept. 2006.
- [2] IEEE 802.16-2005: IEEE Standard for Local and Metropolitan Area Networks – *Part 16: Air Interface for Fixed and Mobile Broadband Wireless Access Systems – Amendment 2: Physical Layer and Medium Access Control Layers for Combined Fixed and Mobile Operation in Licensed Bands*, Feb. 2006.
- [3] IEEE P802.11 Wireless LANs, "Joint proposal: High throughput extension to the 802.11 standard: Phy, Tech. Rep. IEEE 802.11-05/1102r4, January 2006.
- [4] K. Higuchi, H. Kawai, N. Maeda, and M. Sawahashi, "Adaptive Selection of Surviving Symbol Replica Candidates Based on Maximum Reliability in QRM-MLD for OFCDM MIMO Multiplexing", Proc. of IEEE GLOBECOM 2004, pp. 2480 – 2486, vol. 4, Nov. 2004.